

See discussions, stats, and author profiles for this publication at: <https://www.researchgate.net/publication/281067661>

Onboard Flow Sensing in a Quad Rotor Biplane Micro Air Vehicle for Transition between Hover and Steady-Level Flight

Conference Paper · January 2015

CITATIONS

2

READS

154

3 authors:



Vikram Hrishikeshavan

University of Maryland, College Park

42 PUBLICATIONS 161 CITATIONS

[SEE PROFILE](#)



Inderjit Chopra

University of Maryland, College Park

470 PUBLICATIONS 7,751 CITATIONS

[SEE PROFILE](#)



Derrick Yeo

University of Maryland, College Park

27 PUBLICATIONS 69 CITATIONS

[SEE PROFILE](#)

Some of the authors of this publication are also working on these related projects:



Unsteady Two-dimensional Airfoil Characteristics at Low Reynolds Numbers (10^4 - 10^5) [View project](#)



smart structures [View project](#)

Onboard Flow Sensing in a Quad Rotor Biplane Micro Air Vehicle for Transition between Hover and Steady-Level Flight

Vikram Hrishikeshavan

vikramh@umd.edu

Assistant Research Scientist

Derrick Yeo

derrickwyeo@gmail.com

Postdoctoral Research Associate

Inderjit Chopra

chopra@umd.edu

Alfred Gessow Professor and Distinguished

University Professor and Director

Alfred Gessow Rotorcraft Center

Department of Aerospace Engineering

University of Maryland, College Park, MD 20742.

ABSTRACT

While multi-mode vehicles promise improved mission versatility, the transition between different flight modes poses challenges to autonomous flight control. This paper presents an onboard flow-sensing strategy intended to support the autonomous control of a novel quad rotor biplane micro air vehicle, which consists of four propellers with wings arranged in a biplane configuration. An instrumented version of this vehicle concept is built and guided through a series of pitch transitions on a restricted degree-of-freedom test stand. Discrete chordwise stations at a particular spanwise location are instrumented with differential pressure sensors to monitor the aerodynamic state during transition. A custom designed orthogonal airspeed probe measures air velocity components parallel and normal to the wing. Linear transition pitch rates between 8 and 400 deg/s were initiated from steady forward-flight airspeeds between 2.5 m/s and 4 m/s. For all these conditions, significant suction pressures were momentarily generated when a transition command is initiated, with progressively diminishing pressure peaks from the leading edge to trailing edge. The effects of various transition speeds suggest that at high pitch rates achievable with differential thrust control (> 50 deg/s), it is possible for the vehicle to complete a cruise-to-hover transition before experiencing non-linear drop in aerodynamic loads at high angles-of-attack. Additionally, the aerodynamic loads can be quickly directed along the flow aligned direction so that the large transient forces generated by the unsteady aerodynamics serve to decelerate the vehicle instead of inducing undesired climb-rates. A real-time stall detection method using measurement of magnitude and time derivative of suction pressure is proposed, which will be used to augment the inertial controller during transition as part of future work.

INTRODUCTION

There is a significant interest in the development of micro aerial platforms that have the ability to hover and travel fast because of their requirement to perform multiple missions such as health monitoring, surveillance, and payload delivery. In order to combine the hover abilities of a rotary wing vehicle with the rapid deployment capabilities of a fixed-wing aircraft, many hybrid concepts such as tail-sitters, tilt-rotors and tilt-wing (Refs. 1–8) have been explored in the past. In the present study, a quad rotor biplane (QBP) configuration is considered (Ref. 8). The main advantages of this concept are: the pitching moments to achieve transition are generated en-

tirely by differential rotor thrust without the use of additional aerodynamic surfaces, and the biplane arrangement provides additional compactness and maneuverability.

Of major importance is the development of suitable transition flight controllers for these small scale UAVs. Transition between rotor-borne and wing-borne flight modes implies substantial changes in operating regimes, which often involves aerodynamics that is unsteady, nonlinear and sensitive to small changes in flight condition. Previous work in this field has relied primarily on inertial sensors for transition guidance (Refs. 1, 3). However, aerodynamics during transition can be challenging to conventional autopilot systems that rely heavily on inertial instrumentation and linearized control laws. Furthermore, the presence of flow-field variations such as gusts can cause significant motion for such small aerial systems (Ref. 9). This shows the need for real time aerodynamic sensing and control design techniques. Therefore, this paper

Presented at the AHS Specialists Meeting on Unmanned Rotorcraft and Network Centric Operations. Copyright © 2015 by the American Helicopter Society International, Inc. All rights reserved.

introduces a flow-instrumentation system developed to support autonomy of the quad rotor biplane configuration during transition flight.

In the past, researchers have been interested in the precision landing of small fixed-wing vehicles on vertical surfaces. ‘Perching’ has been described as a high angle-of-attack approach with the purpose of using high-drag, separated flow for aerodynamic braking in support of a short or precise landing (Ref. 10). Green and Oh (Ref. 1) appear to be the first ones to develop a linearized transition controller for small, fixed-wing aircraft switching between cruise to hover using inertial measurements. High angle of attack aerodynamics were avoided through rapid pitch maneuvers, leveraging the small scale and low mass of these vehicles. A similar approach was featured in a transition study that demonstrated fixed-wing perching capabilities indoors (Ref. 3). In an outdoor transition study between cruise and hover, noticeable altitude excursions were observed (Ref. 11). Onboard flow sensing and instrumentation for force and moment estimation during transition has been previously explored (Ref. 12), where a linearized control law was augmented with onboard air data measurements using stall detection logic to trigger mode changes. Other real-time flow diagnostic experiments were also conducted such as the separation detection on high performance aircraft by studying the signal from micropores mounted across the airfoil (Ref. 13).

The objective of this paper is to systematically develop and extend onboard flow sensing research to carry out the transition of the quad rotor biplane which will utilize real time inertial measurements augmented with aerodynamic state information. This is studied using a tethered reduced DOF (degree-of-freedom) test-bed that is used to simulate the quad rotor biplane in transition flight. The first section provides an overview of the vehicle design, its operating modes and results from transition flight testing. Following this, the onboard flow sensing instrumentation that can be applied for real-time aerodynamic state measurements on small scale MAVs will be described. The effect of different transition speeds on the pressure measurements over a given airfoil section are systematically studied. From these observations, a stall detection logic is presented. Finally, using the same instrumentation, the ability to detect gusts in real time is presented, which can be used to enable the vehicle to handle gusts in a more efficient manner in the future.

VEHICLE DESIGN AND FLIGHT TESTING

Conceptual design and modes of flight

The conceptual design of the vehicle is shown in Fig. 1. Two counter-rotating propeller pairs are arranged in a quadrotor configuration. Two wings are affixed below each pair of rotors through a set of airfoil shaped attachments. Vertical take-off and landing operations are performed in helicopter mode. The pitch moments required to perform transition are generated through differential RPM settings between the front and aft sets of propellers. As the vehicle enters a horizontal flight

mode at sufficiently high speeds, flight loads are transferred to the wings. One of the main advantages of this configuration is that the quadrotor control system is retained in both hover and forward flight modes, requiring no redundant actuation systems. To understand how control is achieved at these different modes, consider the schematic shown in Fig. 2. The pitch, roll and yaw axes are defined based on the inertial frame in hover mode and are assumed invariant in transition. Therefore it can be seen that as the vehicle transitions from hover to forward flight, the inputs necessary for roll and yaw commands are simply exchanged with respect to the body frame of reference.

Figure 3 shows the assembled vehicle. The wings were constructed from low density polyurethane foam using a high lift low Reynolds number airfoil (FX-63). The wing chords were aligned in the same plane as the propeller axis by lightweight airfoil shaped attachments. The gross weight of the vehicle is about 250 grams. The wing span is 19” with an aspect ratio of 4.8 and the wings are placed about 11” apart. The battery and onboard microcontroller are placed at the center of the vehicle. For propulsion, a set of 2000 kV Hextrontix Brushless outrunner motors were used in conjunction with Turnigy 6-A electronic speed controllers.

Transition Control and Flight Testing

For onboard attitude stabilization and transition guidance, a custom lightweight micro robotic automation platform, ELKA, is incorporated as shown in Fig. 4. It consists of an ARM Cortex-M4 microcontroller, a 9 DOF inertial measurement unit with integrated gyros, accelerometers and magnetometers, and a radio transceiver for wireless communication tasks. It enables onboard computation of vehicle attitude and implementation of appropriate feedback controllers with a stabilization rate of 1000 Hz. Outer loop pilot control can be provided for translational positioning of the vehicle.

Since the vehicle undergoes large changes in pitch angles of up to 90 degrees, a feedback controller was implemented using attitude estimation in quaternion form. The control system development and implementation is described in further detail in (Ref. 14). Free flight transition is performed with the vehicle initially being flown in hover mode from which the pilot issues a pitch-forward command. The throttle is held close to the hover value throughout the transition. The vehicle transitioned smoothly and quickly from helicopter to forward flight mode within 1-2 seconds. It proceeded in forward flight before transitioning back to hover with a pitch-back command issued at a steady throttle setting. This sequence of these events is shown in Fig. 5. During this maneuver, it was generally observed that an excess lift was generated as the vehicle returned to a hover attitude, resulting in altitude gain throughout the transition.

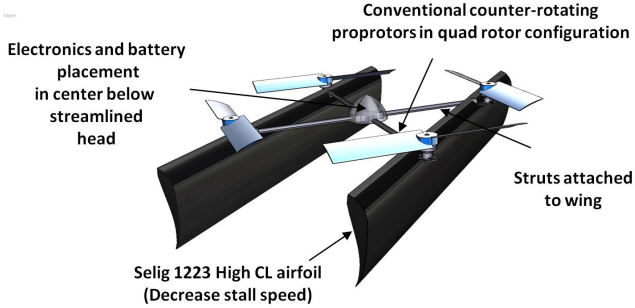


Fig. 1: Conceptual design of quad rotor biplane MAV

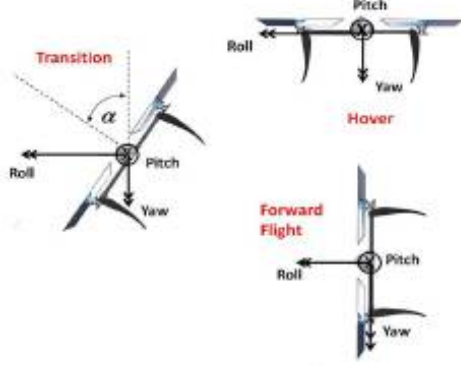


Fig. 2: Frames of reference in hover, transition and forward flight mode: inertial axes-fixed

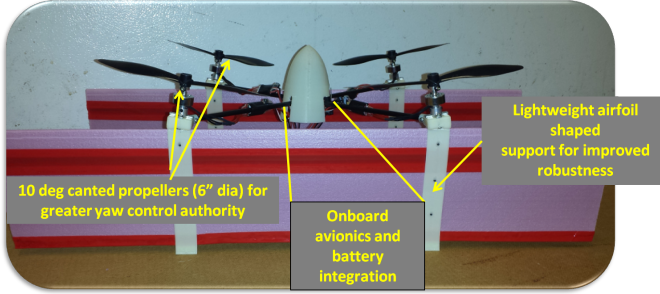


Fig. 3: Integrated 250 gram quad rotor biplane MAV

ONBOARD FLOW SENSING

Objective

As seen from Fig. 5 the transition can be achieved through inertial based feedback alone while ignoring the aerodynamics in transition mode. However, there are limitations to this approach in practical situations where the flight conditions may not be steady, such as transition from forward flight to hover. Figure 6 also describes a scenario where inertial based feedback alone is insufficient to achieve steady transition without changes in altitude. Furthermore, a typical maneuver from hover to level flight may involve progression of the wing flow through stall. While these issues could be partially mitigated by carefully regulating the throttle of the rotors, there needs to be a method to sense these aerodynamic state changes that can then be used to augment the inertial flight controller. For example, if a loss of lift on the wing is detected, the controller can modulate propeller thrust and pitching moment to maintain equilibrium flight. Due to these factors, it appears important to investigate techniques for onboard flow sensing. In order to achieve this, the work is conducted as follows: (1) select testing scheme to study vehicle transition maneuvers in a repeatable manner, (2) explore instrumentation necessary to carry out onboard flow sensing viable for a lightweight MAV, (3) study effects of transition rates on aerodynamic state of the wing, and (4) arrive at guidelines for detecting aerodynamic state changes under unsteady flight conditions such as during transition and presence of gusts. Future work will include

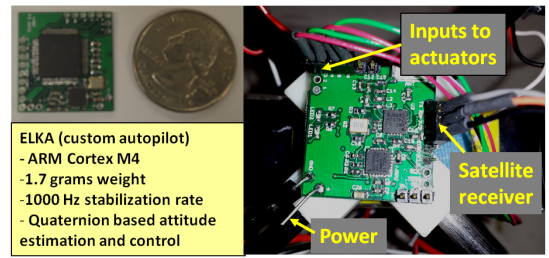


Fig. 4: Implementation of custom autopilot on vehicle for flight testing

augmenting the inertial flight controller with the aerodynamic information and flight testing.

Transition Test Apparatus

In order to characterize the onboard flow sensing for real time feedback, it is important to test the system in a controlled environment. One possible method could be mounting the vehicle, which is free to rotate in pitch degree of freedom, in front of an open jet wind tunnel. Now, it should be noted that there is a very clear dependence between vehicle pitch angle and forward velocity. Typical operation of the wind tunnel does not allow for modulation of flow velocity based on vehicle pitch angle. Even if so, the response time of the wind tunnel for a given input change is more than 3 seconds, which renders an approximate recreation of transition flight less applicable. Alternatively, a fan-bank setup can be considered as shown in Fig. 7. Here the vehicle is mounted on a pitch bearing setup in front of bank of fans, which have a high bandwidth. By pre-determining a velocity variation with pitch angle, the fans can generate increasing velocity as the vehicle transitions from hover to fixed-wing mode (Ref. 14). However a very clear disadvantage with this setup is that the velocity profile is not uniform and the velocity variation with pitch angle may not be representative of free flight transition. Therefore a unique test setup, which draws inspiration from verti-bird toys manufactured in the 1970s, is constructed as shown in Fig. 8. It consists of the vehicle mounted on a pitch bearing, tethered to

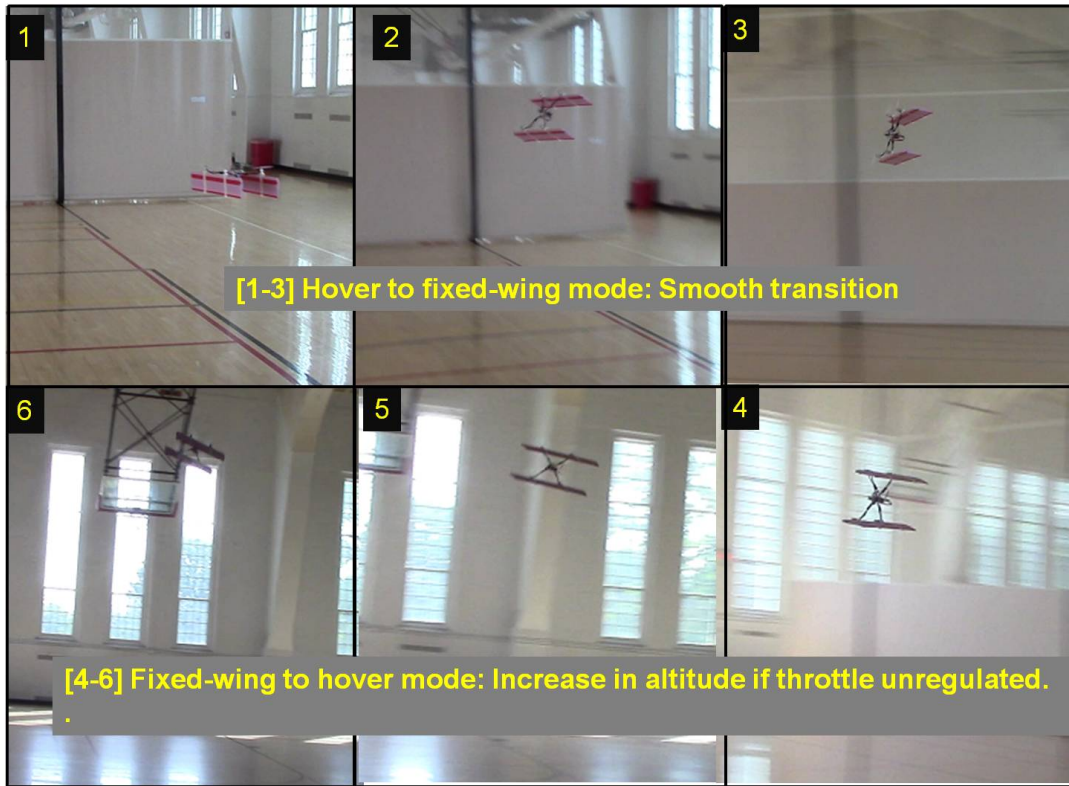


Fig. 5: Transition flight testing of quad rotor biplane from hover to forward flight and back to hover

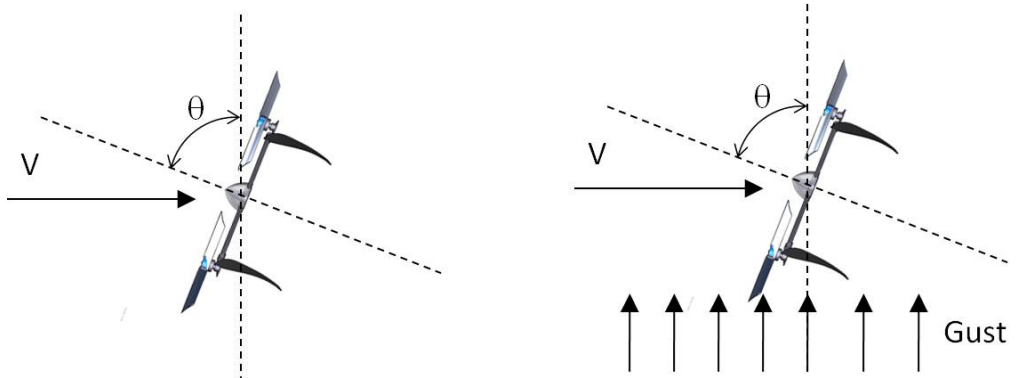


Fig. 6: Limitation of inertial-only based controllers in presence of flow disturbances

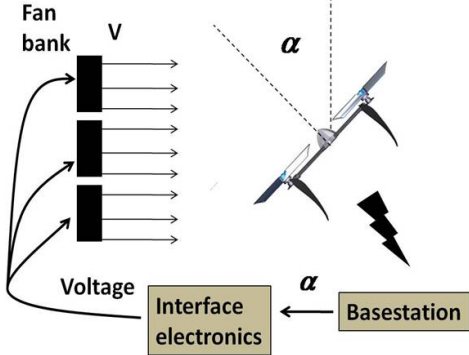


Fig. 7: Schematic of a fan-bank setup to simulate varying dynamic pressure as vehicle transitions from hover to forward flight mode.

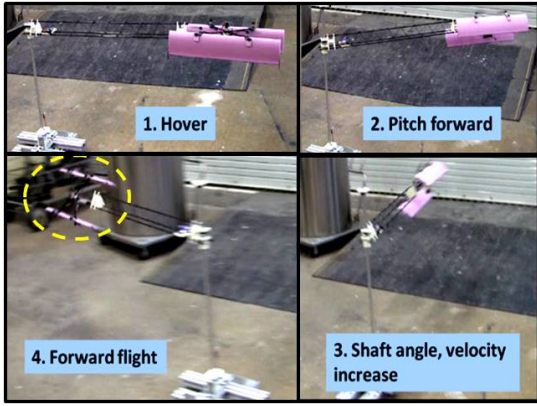


Fig. 9: A representative transition flight of quad biplane undergoing transition in the merry-go-round (MGR) stand

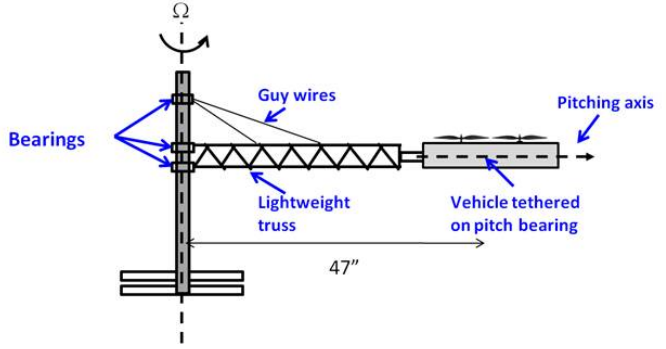


Fig. 8: Merry-go-round (MGR) stand : the vehicle is attached to the truss on a pitch bearing. It propels itself and rotates about the central support structure.

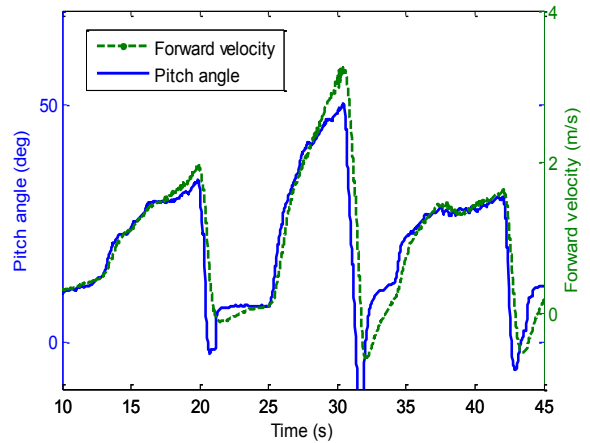


Fig. 10: Variation of pitch angle and forward velocity

a lightweight truss which can rotate about a central shaft. The main advantage of this setup is that the tethered aircraft will be able to change its own free stream velocity through pitch angle variation which is the closest representation of transition in free flight. In this way, the flow sensors can be independently tested for different throttle and pitch angle settings. The lightweight truss on the MGR stand is constructed from 0.2 carbon fiber tubes and 0.02 carbon fiber rods which result in a lightweight structure with minimal inertia. The central rotation axis and support structure are constructed from aluminum. A guy-wire support is also provided to offload the bending moments experienced by the truss. A Hall-effect sensor and gyro are mounted near the central bearing to measure the rotation rate of the truss. In this manner, the tangential velocity at a given location of the vehicle can be estimated. Figure 9 shows a representative flight test where the vehicle is commanded in hover followed by a transition command to forward flight. As shown in Fig. 10, a commanded pitch angle results in a corresponding forward velocity with minimum time delay.

Flow Sensing Instrumentation

The primary objective of the study is to develop a flow-sensing instrumentation scheme and use that methodology to understand the aerodynamic state information on the wings of the quad biplane during transition from forward flight to hover and vice versa. The transition maneuver is studied using a single-wing configuration that is self-propelled and controlled using a pair of counter rotating propellers (Fig. 11). The instrumented wing and flow sensors are located outside the propeller wash region. This configuration allows the fundamental behavior of the aerodynamic instrumentation to be studied during transition while retaining key control system characteristics. Further development of the instrumentation methodology to accommodate the complex aerodynamic interactions found on the quad biplane platform is planned as part of future work. The single wing is instrumented with pressure ports at four different chord stations ($0.18c$, $0.3c$, $0.53c$ and $0.713c$) as shown in Fig. 12. The pressure lines were fabricated from a combination of nylon and tygon tubes that were approximately $0.0625''$ thick. These were embedded into slots that were machined along the wing span and covered using acrylic

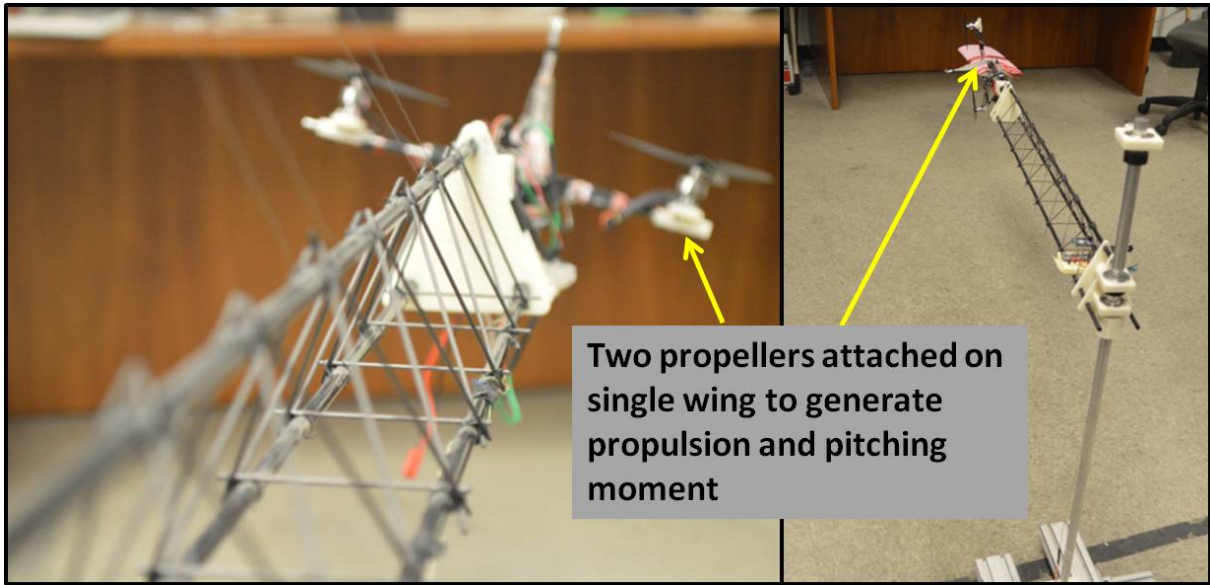


Fig. 11: Approximating quad biplane configuration as a single wing with two propellers that are offset to generate thrust and pitching moment.

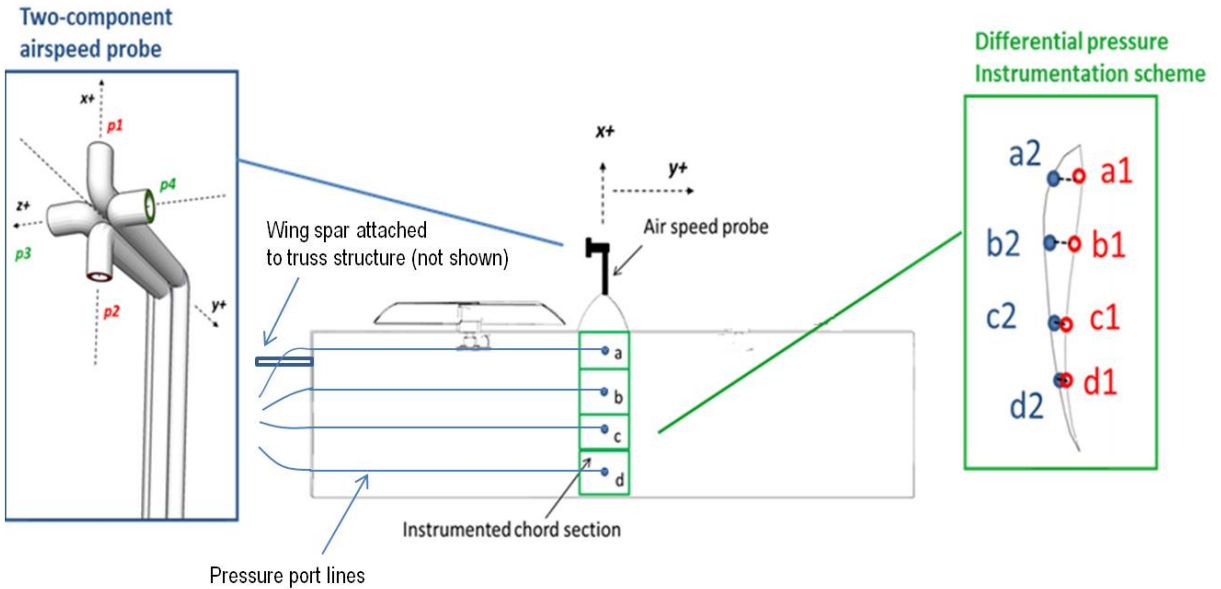


Fig. 12: Location of air speed probe and pressure ports on wing for flow sensing.

tape. Each chord location consists of two pressure ports along the top and bottom surface of the wing. These ports were then routed along the wing and connected to a series of differential pressure sensors. The analog voltage outputs from the Honeywell HSCDRR1NDAA3 differential pressure sensors were connected to four 12 bit Analog/Digital converters on the flight control board (ELKA), and were sampled at 2 kHz. The basic data acquisition and flow instrumentation setup is shown in Fig. 13. A custom designed orthogonal air-speed probe (Ref. 15) measures air velocity components parallel and normal to the wing. The probe is constructed from aluminum tubes bent to shape before being joined. The geometry and pressure-port designations are shown in Figs. 12

and 14. The port configuration enables bi-directional velocity measurements along each orthogonal axis. By considering longitudinal and vertical velocity components, both air-speed and angle of attack can be reliably measured in all flight modes. The free-stream velocity vectors, \mathbf{u} and \mathbf{w} , along the body-fixed x and z directions, can be computed as described in Eqns. 1 and 2

$$u = K_u \sqrt{\frac{2K_b(P_1 - P_2)}{\rho}} \quad (1)$$

$$w = K_w \sqrt{\frac{2K_b(P_1 - P_2)}{\rho}} \quad (2)$$

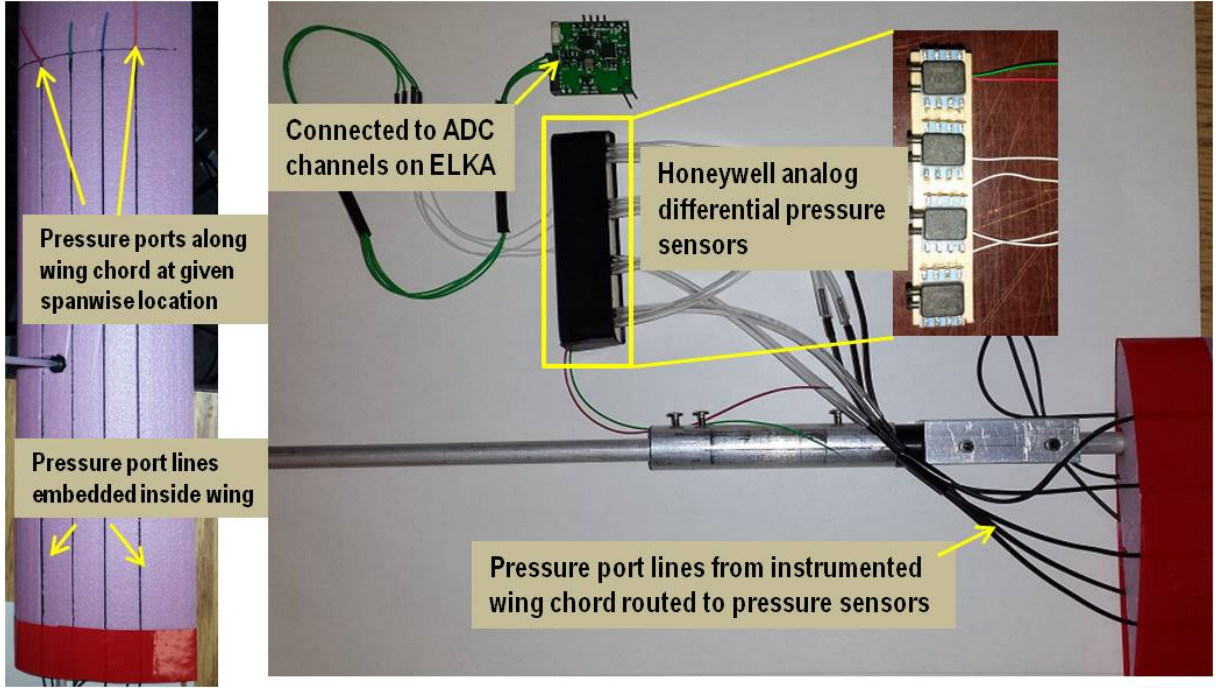


Fig. 13: Onboard flow sensing instrumentation. The pressure ports are connected to differential pressure sensors which are sampled by ADC channels on ELKA at 2000 Hz.

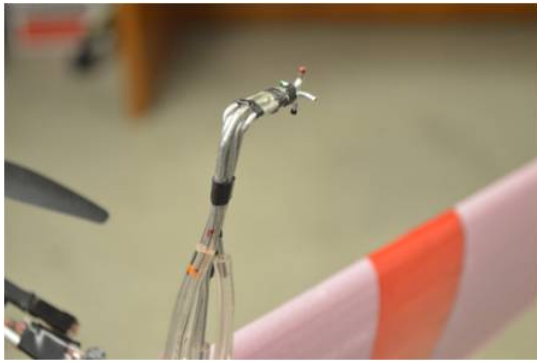


Fig. 14: Unique two component flow probe to measure velocity components parallel and normal to wing chord

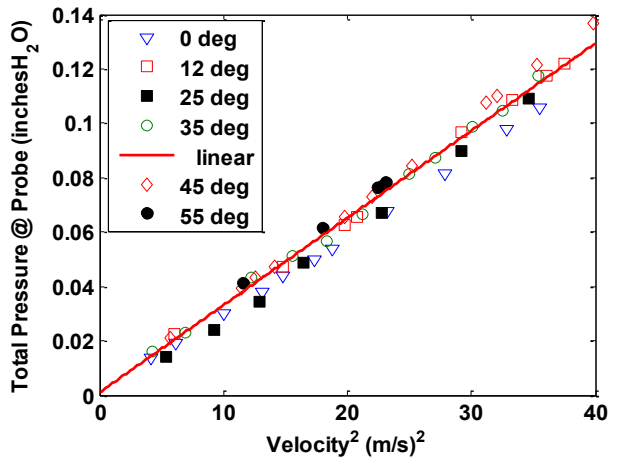


Fig. 15: Wind tunnel calibration of flow probe sensor. Measured pressure invariant with angle of inclination

where K_u , K_w and K_b are calibration constants and $P1, P2, P3$ and $P4$ denote the pressure at the tips of the multi-hole probe as defined in Figure 12. Due to symmetry in flow probe design, the value of calibration constants are equal, $K_u = K_w$. Therefore the total velocity magnitude (V) and angle of attack (α) can be computed as,

$$V = \sqrt{u^2 + w^2} = K_u \sqrt{\frac{2K_b[(P_1 - P_2) + (P_3 - P_4)]}{\rho}} \quad (3)$$

$$\alpha = \tan^{-1} \frac{w}{u} \quad (4)$$

For this application, the probe is connected to a pair of HSC-DDR1NDAA3 differential pressure sensors. The probe and sensor package was calibrated using an automated rotating stage in the UMD open-test-section wind tunnel at airspeeds between 0 m/s and 8 m/s. Figure 15 shows the calibration results of the flow probe at different angles of attack and air speed. It can be seen that the total velocity measured by the flow probe remains unaffected by angle of attack as predicted from Eq. 3. Using these calibration results, the velocity and angle of attack measured by the flow probe were compared with inertial and Hall sensors on the MGR stand with satisfactory agreement as shown in Figs. 16 and 17. The wing

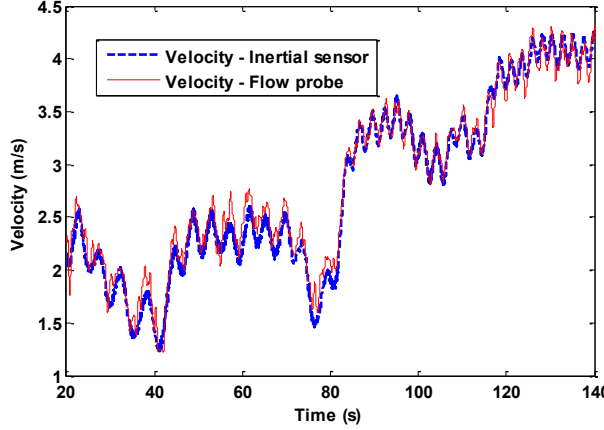


Fig. 16: Comparison of measured velocity between flow probe and inertial based sensor

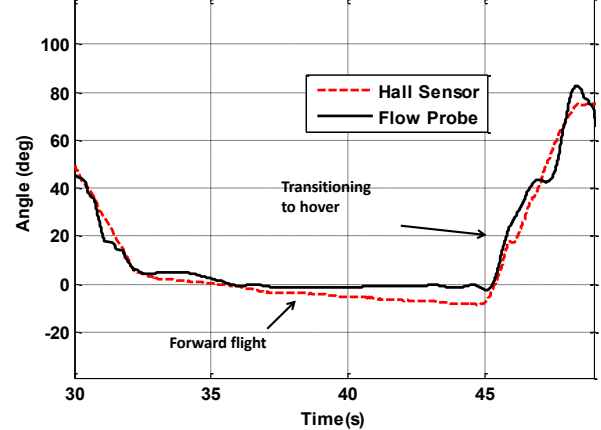


Fig. 17: Comparison of measured angle of attack between flow probe and hall sensor during a transition maneuver

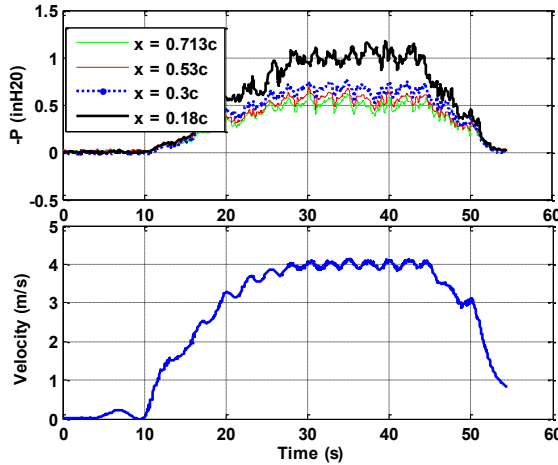


Fig. 18: Time history of suction pressure at different chordwise locations at 10 deg angle of attack

was then fixed at different pitch settings on the MGR stand (Fig. 11) and was propelled around the axis to generate suction pressure at the various chordwise pressure ports. Figure 18 shows the variation of suction pressure as the wing was rotated from rest to upto 4 m/s and back at an angle of attack of 10 degrees. As expected, the chordwise stations closer to the leading edge generate higher suction pressures. This chordwise pressure distribution will change as the angle of attack is increased (Fig. 19). By comparing this distribution, an approximation of certain events such as wing stall can be estimated. The next section discusses an extension of this testing scheme where dynamic pitching is introduced to simulate transition modes from hover to forward flight.

Transition Rate Testing

As described previously, the MGR stand allows the system to propel itself between hover and forward flight in a repeatable

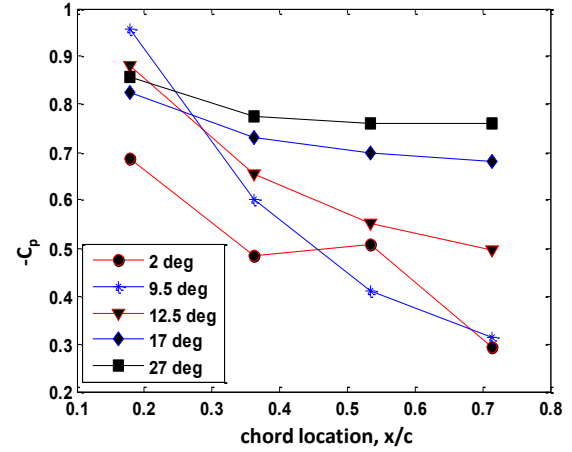


Fig. 19: Variation of non-dimensional pressure with chordwise location at various angles of attack

fashion. This enabled a series of tests to investigate the variations in chordwise pressure measurements during transition at different rotation rates and from different initial airspeeds. These maneuvers are defined by linear ramps in pitch angle and are governed by the onboard controller. Linear pitch rates between 8 and 400 deg/s were initiated from steady forward-flight airspeeds between 2.5 m/s to 4 m/s. Figure 20 shows a schematic of the transition maneuvers that were realized.

Results

Pressure distribution along wing chord:

A variation in pressure along the instrumented chord during a 40 deg/s transition at 3.7 m/s is shown in Fig. 21. It is noted that the suction pressure is plotted on the y-axis, so a positive value indicates lift. These time histories exhibit the same trends observed in all other test cases and are thus considered representative results. The following salient observations can be made:

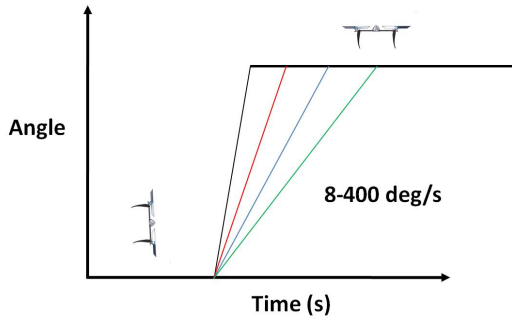


Fig. 20: System tested at different rates of transition from forward flight to hover

- (a) Regardless of pre-existing conditions in forward flight, a significant suction pressure is momentarily generated when a transition command (from axial flight to hover) is initiated throughout the wing chord that eventually reduces to ambient pressure as the wing enters a vertical hover state.
- (b) At the beginning of transition, a local peak is observed near the trailing edge which is followed by a peak at $x = 0.53c$. This suggests that a trailing edge vortex is initially shed and induces pressure variations as far as 70% of the chord.
- (c) Following the successive local suction pressure peaks near the latter half of the wing chord, a large peak is observed close to the leading edge. This is then succeeded by peaks at $x = 0.3c$, $0.53c$ and $0.713c$. Since the influence of a passing vortex greatly increases local suction pressure gradients, this observation suggests that a leading edge vortex is shed and its influence can be measured as it convects downstream during the transition maneuver.

These trends are consistent with the dynamic stall effects encountered by rapidly pitching airfoils. (Refs. 16, 17).

Effect of ramp rate:

Since all wing chord stations exhibit suction pressure peaks upon transition, only the pressure state near the leading edge ($x=0.18c$) is shown for purposes of clarity. Figure 22 shows the suction pressure variation at ramp rates of 10, 20, 40 and 80 deg/s. It can be seen that at all ramp rates, a significant pressure peak is measured shortly after the transition is initiated. After that, the time taken for the pressure to decay back to ambient pressure levels is dependent on the ramp rate. For example, a high suction pressure is sustained for a longer time for a ramp rate of 10 deg/s (Fig. 22(a)) when compared with 80 deg/s (Fig. 22(d)).

By comparing the magnitudes of the pressure peaks, it can be observed that the magnitude of the pressure peak increases with ramp rate. Figure 23 shows the pressure peak magnitude (P_{peak}) increasing with higher initial forward flight velocities (V). Based on the measurements from the different ramp rates and forward speed tests, it was observed that pressure peak

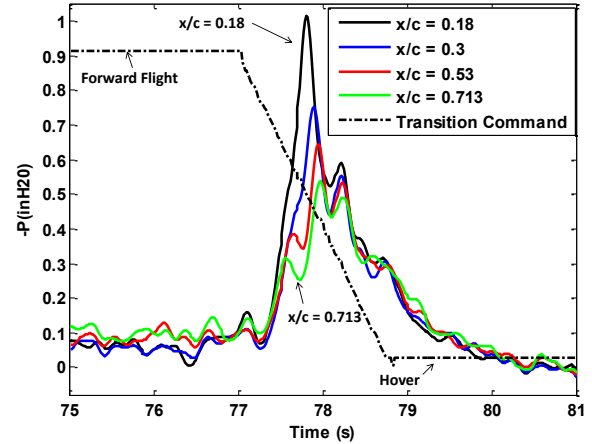


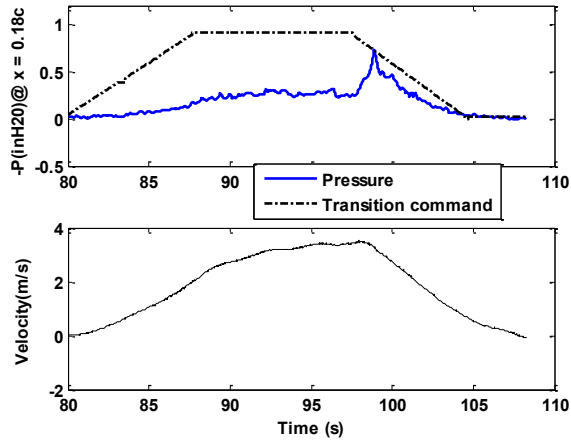
Fig. 21: System tested at different rates of transition from forward flight to hover

magnitudes scaled approximately with the third power of velocity, $|P_{peak}| \propto V^3$. Using this approximation, the pressure peak magnitude is compared for various rates in Fig. 24. It can be clearly seen that as the transition speed increases, the suction pressure peak increases until it mostly asymptotes at very high ramp rates (400 deg/s). Even though there is an increase in pressure peak with transition speed, it is mild. For example, for a 20x rise in ramp rate, there is only a 35% increase in pressure peak.

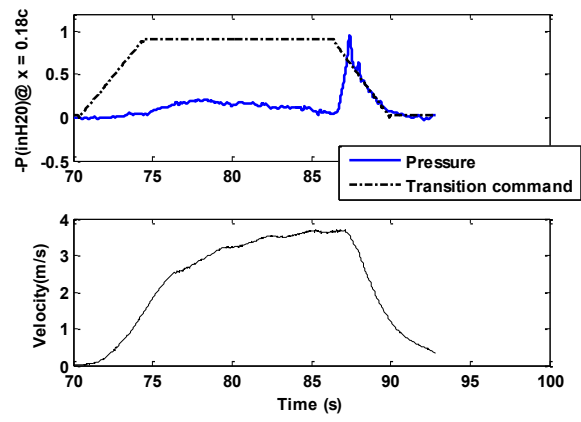
Implications on autonomous transition strategies:

These reduced-degree-of-freedom transition experiments were conducted to gain insight on the unsteady aerodynamic effects encountered during self-propelled pitch rotations. Specifically, nonlinear phenomena such as stall could drive requirements for effective transition guidance. The delay between initial rotation and the occurrence of the first measured pressure peak was identified as a key parameter that might impact future control design. This is referred to as Δt (Fig. 25) and is plotted in Fig. 26 for different rotation rates. It is noted that Δt decreases with increasing rotation rate as expected, but approaches a minimum value near 50 deg/s. Beyond 50 deg/s, significant increases in rotation rate result in a marginal decrease. This suggests the vehicle might be able to complete a cruise-to-hover transition before experiencing a non-linear drop in aerodynamic forces if it rotated rapidly enough. This observation supports the intuition expressed by (Refs. 1, 3) that smaller vehicles could ‘bully their way through stall’ through transition maneuvers that took advantage of high rotation rates.

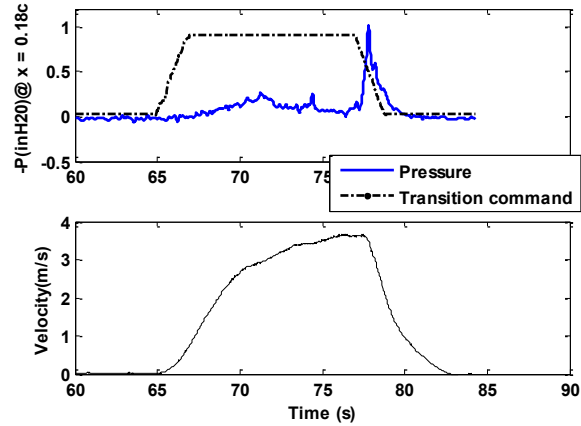
For example, a gradual rotation rate of 10 deg/s would imply a cruise-to-hover maneuver that lasts 9 s with stall occurring 1.7 s after the transition is initiated. Such a controller would need to cope with the onset of stall and the subsequent challenges of high angle-of-attack aerodynamics. Alternatively, a rapid 200 deg/s rotation rate at this Reynolds number results in a transition that only lasts 0.45 s with ‘stall-peaks’ occurring after the transition has been completed at 0.6



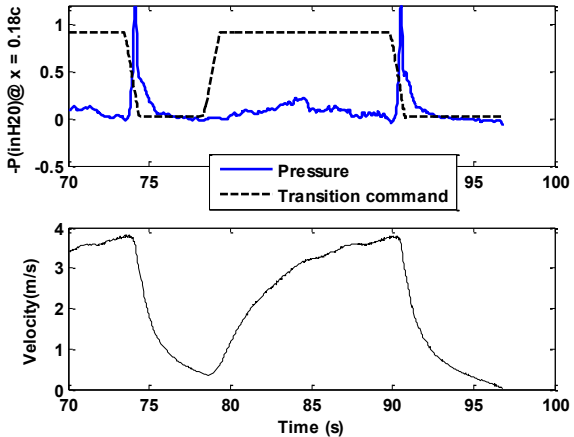
(a) 10 deg/s



(b) 20 deg/s



(c) 40 deg/s



(d) 80 deg/s

Fig. 22: Pressure distribution at $x=0.18 c$ for different transition speeds

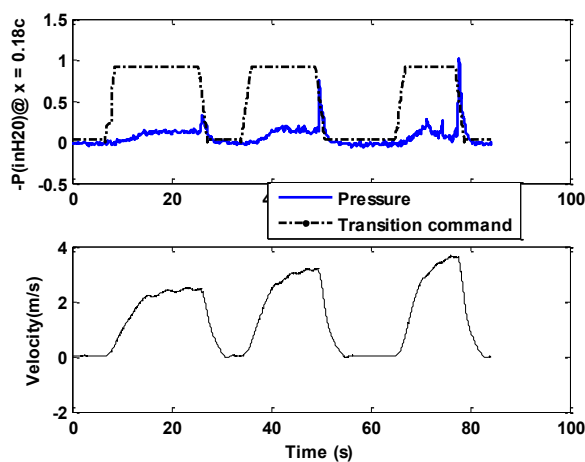


Fig. 23: Pressure peak variation at different forward flight speeds

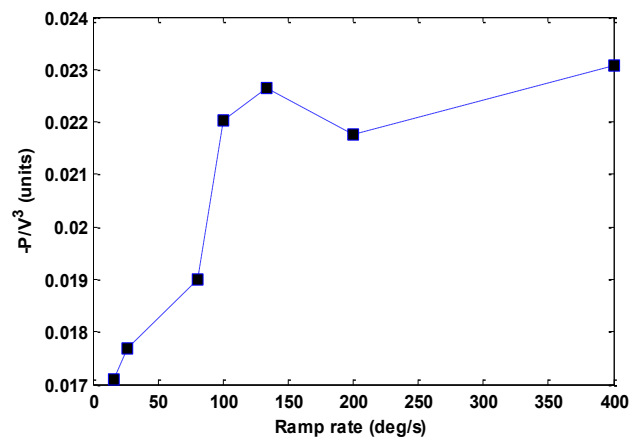


Fig. 24: Variation of pressure peak magnitude as a function of ramp rate

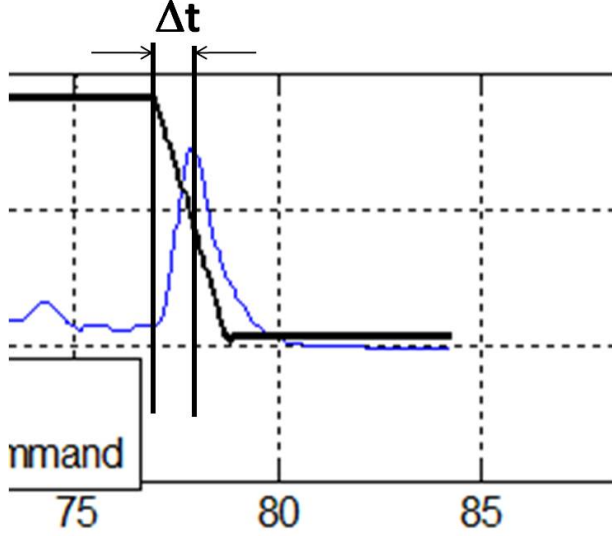


Fig. 25: Occurrence of suction pressure peak a short time, Δt , after transition command

s. While the aerodynamic loads encountered during a rapid transition will be large, these restricted-motion tests suggest that they may be more linear and thus be more suitable for the small quad biplane configuration.

In addition to minimizing the non-linearity of the aerodynamic loads experienced by the vehicle during transition, it is hypothesized that a rapid transition may also reduce some of the altitude excursions observed during milder transition maneuvers (Fig. 5). During transition at a rotation rate of 10 deg/s (Fig. 22(a)), the vehicle takes 9 s to decelerate from forward flight and rotate to a hover attitude. Pressure measurements indicate that the wing generates considerable aerodynamic lift as it rotates. When coupled with the vertical component of rotor thrust, the additional lift generated during the rotation can lead to undesired altitude excursions. A transition maneuver that rapidly flips the wing into a vertical orientation can quickly direct the aerodynamic loads along the flow aligned direction and rapidly decelerate the vehicle. By avoiding a prolonged deceleration phase, this would preclude the need for additional rotor thrust control through aerodynamic feedback. This kind of aerodynamic braking effect has also been observed on perching aircraft (Ref. 10).

Stall Detection

Previous results showed that as the wing transitions from cruise to hover, significant non-linear aerodynamic phenomena occur - most notably the appearance of distinct suction pressure peaks throughout the wing chord. It is envisaged that the ability to detect stall in real-time transition maneuvers will aid traditional-inertial based controllers in improving cruise-to-hover transitions. Detecting stall in real-time may involve monitoring multiple factors. A few of them are: (1) loss-of-lift, (2) uniform chordwise suction pressure distributions below a certain threshold (Fig. 24), and (3) cascading suction

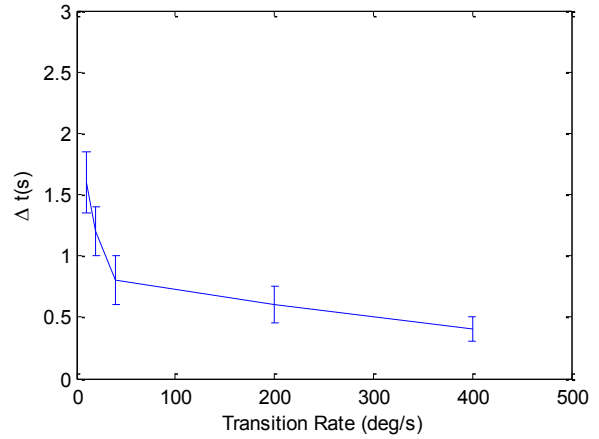


Fig. 26: Variation of Δt with transition speed

pressure peaks along wing chord. While factors (1) and (2) are established during static stall, cruise-to-hover transition maneuvers involve airfoil pitching which undergo dynamic stall (Ref. 16). As we noticed earlier, these are always accompanied by pressure peaks at various chordwise locations. Since the suction pressure peak close to the leading edge has the largest magnitude and occurs first (Fig. 21), it is proposed that an aerodynamic state change (such as wing-stall during transition) may be observed by simply detecting the pressure peak close to the leading edge. This has the additional advantage that only instrumentation of a single or few pressure ports close to the LE may be necessary, as well as reducing the time delay between occurrence of stall and its subsequent detection. Based on this approach, two parameters can be used to detect the aerodynamic state change: suction pressure and slope of suction pressure. These parameters would indicate a change in aerodynamic state once they rise beyond a certain threshold. It should be noted that these thresholds will depend on various factors such as vehicle weight, wing area and flight speed. Since the vehicle parameters can be obtained a priori and flight speed measured in real time using the flow probe sensor, these thresholds can be empirically chosen through flight testing. The slope of pressure can be calculated as,

$$\dot{P}_t = \Delta t (P_t - P_{t-1}) \quad (5)$$

It can be appreciated that the above difference can lead to significant noise. Additionally, 12-bit samples of pressure data may not be sufficient to obtain sufficient resolution between successive pressure measurements. Hence, it became necessary to calculate the slope as,

$$\dot{P}_t = \frac{\Delta t (P_t - P_{t-n})}{n} \quad (6)$$

In order to efficiently implement this without straining embedded processor memory and affecting the feedback loop rate, a

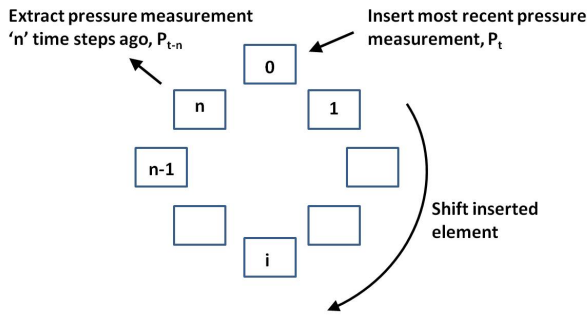


Fig. 27: Circular buffer implementation to compute difference between pressure measurements at time ‘ t ’ and ‘ $t-n$ ’

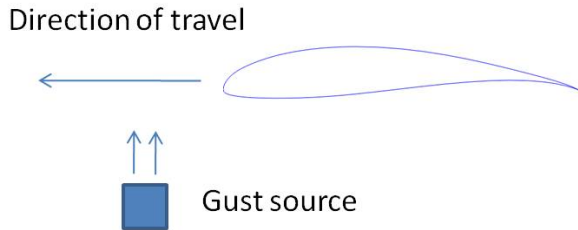


Fig. 29: Schematic of gust detection experiment: wing is rotated through a vertical gust source. This gust is detected by the flow probe sensor and embedded pressure ports on the wing

circular buffer method was incorporated as shown in Fig. 27. For the present case, sufficient slope resolution was obtained for $n=10$.

Using appropriate threshold settings selected for the test stand, this framework provided real-time, aerodynamic-state-change indicators during transition and demonstrated the feasibility of a cost-effective method for stall-detection on small UAVs. As shown in Fig. 28, this framework successfully detected stall for multiple transition maneuvers by monitoring the time derivative of pressure measurements taken over the wing. Future work will involve improving the fidelity of this approach and exploring ways to apply this to trigger changes in controller design, selection of gains and actuator thrust modulation.

Gust Detection and Future Work

In addition to enhancing transition control, onboard flow sensing could also provide gust sensing capabilities. Inertial measurements can only indicate the effect of flight disruption after the vehicle has been perturbed, while direct measurements of aerodynamic forcing could offer disturbance information before the vehicle reacts. With flow measurements directly

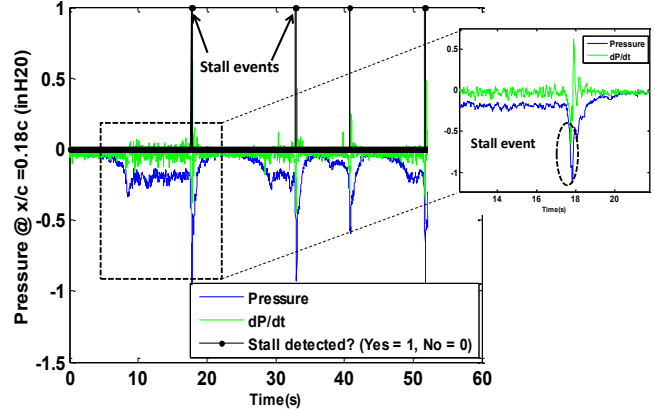


Fig. 28: Real-time detection of stall from measurements of pressure and time derivative of pressure for multiple transition maneuvers

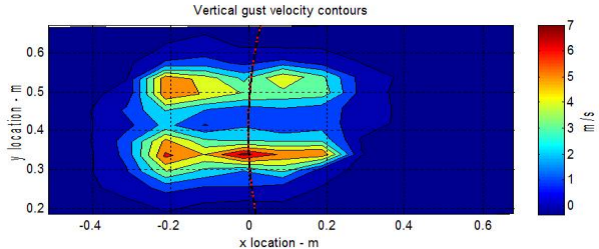


Fig. 30: Vertical flow-field generated by fan with sensor path indicated in red/black dashes.

ahead of the vehicle, an autopilot could predict impending disruptions of the aerodynamic loads experienced by the vehicle. As part of ongoing work, the gust-detection ability of the instrumentation system was evaluated by subjecting the test vehicle to a vertical gust (Fig. 29). A blower-style household fan was used to generate a vertical flow-field in the path of the test vehicle. A contour map of the vertical velocity profile generated by the fan is shown in Fig. 30. The flow survey was conducted using an automated Cartesian robot described in previous work (Ref. 18). The arc drawn across the plot marks the path taken by the flow sensor.

As shown in Fig. 31, the flow disturbance registers on both the wing-mounted sensors and the air-data probe. Being positioned ahead of the vehicle, the airspeed probe is able to detect the updraft before it influences the wing. In these reduced degree-of-freedom tests, the effect on vehicle attitude is minimal. Future work seeks to expand these studies to include the heave degree of freedom on the MGR stand.

CONCLUSIONS

Recently, there is significant effort towards development of multi-role vehicles that can exploit rotary and airplane (prop-rotor) capabilities. While these vehicle configurations provide

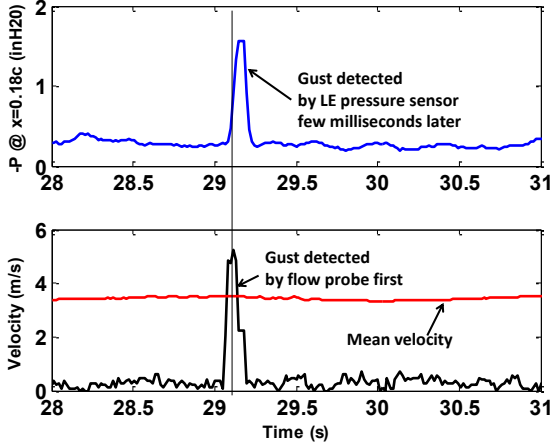


Fig. 31: Gust detection by flow probe (bottom) and embedded pressure sensor (top). The spatial displacement between the flow probe and LE of the wing can be used to detect gust before wing can experience effects of gust.

improved mission versatility, the transition between different flight modes poses challenges to autonomous flight control. This paper examines an onboard flow-sensing strategy to support the transition control of a novel quad rotor biplane micro air vehicle that consists of four propellers with wings arranged in a biplane configuration.

An instrumented version of this vehicle concept that consists of a single wing with two propellers is built and guided through a series of pitch transitions in a restricted degree-of-freedom test stand. The wing is equipped with embedded differential pressure ports at four chordwise locations in conjunction with a custom built orthogonal airspeed probe to measure air velocity components parallel and normal to the wing. A custom autopilot handles real-time analog/digital pressure measurements as well as flight control of the system.

The merry-go-round (MGR) test stand allows the system to propel itself between hover and forward flight. Linear pitch rates between 8 and 400 deg/s were initiated from steady forward-flight airspeeds between 2.5 m/s and 4 m/s and chordwise pressure variations were studied. The following salient observations were made:

1. Regardless of transition rate, a significant suction pressure is momentarily generated when a transition command is initiated. After that, the time taken for the pressure to decay back to ambient pressure levels is dependent on the ramp rate.
2. The magnitude of the pressure peaks progressively diminish from leading edge to trailing edge during transition mode.
3. Pressure peak magnitudes scaled approximately with the third power of velocity, $|P_{peak}| \propto V^3$.
4. A 20 times rise in ramp rate only resulted in a 35% increase in pressure peak.

5. The time spent by the vehicle in non-linear aerodynamic regime is lower for higher transition rates. Additionally a rapid transition maneuver quickly directs the aerodynamic loads along flow aligned direction and can be used to rapidly decelerate the vehicle and minimize altitude excursions.

Based on the pressure measurements, a stall detection method was proposed where an aerodynamic state change (such as wing-stall during transition) can be observed by simply detecting the pressure peak close to the leading edge. Two parameters were used to detect this: suction pressure and slope of suction pressure. This was implemented in real-time and stall-events were captured satisfactorily on representative transition maneuvers. Preliminary gust detection methods were also studied which suggest that the onboard airspeed probe can be used to detect gust and ‘warn’ the controller before the vehicle can experience the effects of gust. Future work seeks to incorporate these onboard flow sensing methods to augment inertial controllers for transition guidance.

REFERENCES

- ¹W. Green and P. Oh, “A MAV that flies like an airplane and hovers like a helicopter,” Proc. 2005 IEEE/ASME International Conference on Advanced Intelligent Mechatronics, 24-28 July Monterey, CA.
- ²Stone, R.H., Anderson, P., Hutchison, C., Tsai, A., Gibbens, P., and Wong, K.C., “Flight Testing of the T-Wing Tail-Sitter Unmanned Air Vehicle,” *Journal of Aircraft*, Vol. 45, No. 2, 2008, pp. 673-685.
- ³Frank, A., McGrew, J.S., Valenti, M., Levine, D., and How, J.P., “Hover, Transition, and Level Flight Control Design for a Single-Propeller Indoor Airplane,” AIAA Guidance, Navigation and Control Conference and Exhibit, Hilton Head, South Carolina, AIAA Paper 2007-6318, 2007.
- ⁴Kubo, D. and Suzuki, S., “Tail-Sitter Vertical Takeoff and Landing Unmanned Aerial Vehicle: Transitional Flight Analysis,” *Journal of Aircraft*, Vol. 45, No. 1, 2008, pp. 292-297.
- ⁵Suzuki, S., Zhijia, R., Horita, Y., Nonami, K., Kimura, G., Bando, T., Hirabayashi, D., Furuya, M., and Yasuda, K., “Attitude Control of Quad Rotors QTW-UAV with Tilt Wing Mechanism,” *Journal of System Design and Dynamics*, Vol. 4, No. 3 (2010), pp.416-428.
- ⁶Hrishikeshavan, V., and Chopra, I., “Design and Control of a Tilt-Wing Micro Air Vehicle in Hover,” American Helicopter Society 68th Annual Forum, Fort Worth, Texas, May 2012.
- ⁷Itasse, M., Moschetta, J.M., Ameho, Y., Carr, R., “Equilibrium Transition Study for a Hybrid MAV,” *International Journal of Micro Air Vehicles*, Volume 3, Number 4, pages 229-245, 2011.

⁸Hrishikeshavan, V., Bogdanowicz, C., and Chopra, I., “Performance and Flight Testing of a Quad Rotor Biplane Micro Air Vehicle for Multi Role Missions,” 55th Structures, Structural Dynamics, and Materials Conference, National Harbor, Maryland, Jan 2014.

⁹Pisano, W., and Lawrence, D., “Control limitations of small unmanned aerial vehicles in turbulent environments,” Proc. AIAA Guidance Navigation and Control Conference, 10-13 August 2009, Chicago Illinois. (AIAA 2009-5909).

¹⁰Wickenheiser,A., and Garcia,E., “Longitudinal Dynamics of a Perching Aircraft,” *Journal of Aircraft* Vol. 43, No. 5 (2002) pp 1386-1392. doi 10.2514/1.20197

¹¹Johnson, E., and Kannan, S., “Adaptive Flight Control for an Autonomous Unmanned Helicopter,” Proc. AIAA Guidance, Navigation, and Control Conference, 5-8 August 2002, Monterey California . (AIAA 2002-4439)

¹²Yeo, D., Henderson, J., and Atkins, E., “An Aerodynamic Data System for Small Hovering Fixed-Wing UAS,” Proc. AIAA Guidance, Navigation, and Control Conference, 10-13 August 2009, Chicago Illinois. (AIAA 2009-5756)

¹³Heller, H., Bliss, D.B., and Widnall, S.E., “Incipient stall detection through unsteady-pressure monitoring on aircraft wings,” *Journal of Aircraft*, Vol. 9, No. 2 (1972), pp. 186-188. doi: 10.2514/3.44328

¹⁴Hrishikeshavan, V., Bawek, D., Rand, O., and Chopra, I., “Control of a Quad Rotor Biplane Micro Air Vehicle in Transition from Hover to Forward Flight,” American Helicopter Society Specialists Meeting on Unmanned Rotorcraft, Scottsdale, AZ, Jan 2013.

¹⁵Yeo,D., Sydney, N., and Paley, D., “Onboard Flow Sensing for Downwash Detection and Avoidance with a Small Quadrotor Helicopter,” Proc. AIAA Guidance Navigation and Control Conference, Kissimmee Florida, January 2015 (AIAA 2015-1769)

¹⁶Visbal, M.R., “Dynamic stall of a constant-rate pitching airfoil,” *Journal of Aircraft* Vol.27 No.5 (1990): 400-407.

¹⁷Walker, J.M., and Seiler, F.J., “Forced unsteady vortex flows driven by pitching airfoils,” AIAA 19th Fluid Dynamics, Plasma Dynamics and Lasers Conference, Honolulu, Hawaii, Jun. 1987 (AIAA-87-1331).

¹⁸Yeo, D., Shrestha, E., Paley, D., and Atkins, E., “An Empirical Model of Rotorcraft UAV Downwash for Disturbance Localization and Avoidance,” Proc. AIAA Atmospheric Flight Mechanics Conference , Kissimmee, Florida, January 2015 (AIAA 2015-1685)